Ciemat
Centro de
Investigaciones Energéticas,
Medioambientales
y Tecnológicas

Miner

A Novel Method for Short Distance Measurements

CIEMAT:
M. G. Fernández
A. Ferrando
M. I. Josa
A. Molinero
J. C. Oller

CSIC:
P. Arce
E. Calvo
C. F. Figueroa
N. García
T. Rodrigo
I. Vila
A. L. Virto

Informes Técnicos Ciemat 867
diciembre, 1998

Informes Técnicos Ciemat 867
diciembre, 1998

A Novel Method for Short Distance Measurements

CIEMAT:
M. G. Fernández
A. Ferrando
M. I. Josa
A. Molinero
J. C. Oller

CSIC:
P. Arce
E. Calvo
C. F. Figueroa
N. García
T. Rodrigo
I. Vila
A. L. Virto

Departamento de Fusión y Partículas Elementales

CLASIFICACIÓN DOE Y DESCRIPTORES

430303; 440800
HIGH ENERGY PHYSICS; REMOTE SENSING; ALIGNEMENT; PARTICLE TRACKS; DISTANCE; ACCELERATORS;

Toda correspondencia en relación con este trabajo debe dirigirse al Servicio de Información y Documentación, Centro de Investigaciones Energéticas, Medioambientales y Tecnológicas, Ciudad Universitaria, 28040-MADRID, ESPAÑA.

Las solicitudes de ejemplares deben dirigirse a este mismo Servicio.

Los descriptores se han seleccionado del Thesauro del DOE para describir las materias que contiene este informe con vistas a su recuperación. La catalogación se ha hecho utilizando el documento DOE/TIC-4602 (Rev. 1) Descriptive Cataloguing On-Line, y la clasificación de acuerdo con el documento DOE/TIC.4584-R7 Subject Categories and Scope publicados por el Office of Scientific and Technical Information del Departamento de Energía de los Estados Unidos.

Depósito Legal: M-14226-1995
NIPO: 238-98-002-5
ISSN: 1135-9420

Editorial CIEMAT

"A Novel Method for Short Distance Measurements"

Fernández, M. G.; Ferrando, A.; Josa, M. I.; Molinero, A. Oller, J. C. (CIEMAT)
Arce, P.; Calvo, E. Figueroa, C. F.; García, N.; Rodrigo, T.; Vila, I.; Virto, A. L. (CSIC)

16 pp. 4 figs. 4 refs.

Abstract:

A new, accurate and unexpensive device for measuring short distances, intended for monitoring in LHC experiments is presented. Data taken with a very simple prototype are shown and performance is extracted.

"Un Nuevo Método par la Medida de Distancias Cortas"

Fernández, M. G.; Ferrando, A.; Josa, M. I.; Molinero, A. Oller, J. C. (CIEMAT)
Arce, P.; Calvo, E. Figueroa, C. F.; García, N.; Rodrigo, T.; Vila, I.; Virto, A. L. (CSIC)

16 pp. 4 figs. 4 refs.

Resumen:

Presentamos un dispositivo preciso y de bajo coste para la medida de distancias cortas. Mostramos medidas tomadas con un prototipo muy sencillo y extraemos sus prestaciones.

1. Introduction

During LHC [1] operation, longitudinal motions ranging from milimiters to a few centimeters are expected in the CMS [2] experiment due to the forces originated by its 4 T solenoid [3]. The CMS alignment system [4] will have to monitor the distances between particular reference points located at several places in the experiment. Carbon fibers tubes or even aluminium bars (whose mechanical properties and dilatation coeficients are well known) can be used for long distances.

For short distances we have tested a new device based on an infrared source and an infrared light to frequency converter. As it will be shown in this document, this SLFCD (Short Distances LFC Measuring Device) has very good properties for its use in LHC experiments (and in fields other than high energy physics) as: acceptable resolution (better than 10 μm), small size (2x2 cm^2 transverse dimensions, 0.5 cm deep, including the integrated electronics) and very low price (less than 20 US$ for the minimal configuration presented here).

In what follows we will present the working principle of the device in section 2. The experimental setup, data analysis and measured performance will be given in section 3. Conclusions will be drawn in section 4.

2. The SLFCD working principle

The device consists in an infrared light source (LED) and an infrared light to frequency converter (LFC). The LFC is a CMOS integrated circuit that combines a silicon photodiode and a monolitic current to frecuency converter. In the simple prototype constructed, LED and LFC are located, together with the electronics, in the same integrated circuit board. The set is complemented with a diffuser (a white painted screen) placed, in front of the device, at a certain distance.

The light emmitted by the LED is diffused by the screen and part of it comes back and is detected by the photodiode. The light intensity is converted into a pulse train output by means of a current to frequency converter. Fig. 1 shows a flowchart of the operation.

The frequency to current converter consists of an operational amplifier integrator, a transistor reset switch, a level detector and a one-shot pulse generator. The integrator produces a ramp with a slope proportional to the photodiode current. The level detector resets the integrator when the ramp reaches a threshold voltage. The cycle is then repeated, producing the frequency signal. The output of the level detector triggers the one-shot pulse generator which provides the fixed-width output pulse.

This type of device has three main advantages:

1) A wide dynamic range of input light.

Typical light sensing elements convert light into signal in the form of current, voltage or resistance. Usually one must use an amplifier of the signal that is interfaced to a digital system through an ADC. In that case one is limited by the supply voltage and the noise.

In the device we propose, the light to frequency converter dynamic range is not limited by the voltage supply and one can get a dynamic range over 100 dB.

2) Immunity to high noise.

Once converted to frequency, the signal is virtually noise immune and can be sent by cables from remote sensors to other parts of the system. For frequency conversion it is not necessary any external component, thus external interferences are avoided and therefore, the signal to noise ratio is very high.

3) Minimum component interface.

The light to frequency converter output interfaces directly with the TTL logic, thus one can get a direct interface to a logic circuit or a microcontroller.

On the other hand, the fact of working in the infrared makes that the signal is practically unaffected by the ambience light.

Variables are the LED intensity and the time window for signal integration (the time used for pulse counting). The counted number of pulses is a function of the distance between the LFC and the diffusion screen.

3. Tests and results

3.1 The experimental setup

The layout of the experimental setup is shown in fig. 2. The device is located on a motorized platform whose movement has a resolution better than 2 μm. The diffusion screen is fixed. The control of the platform motion is made by a board motor controller located in a PC. A precise variable current source is used to power the infrared light source, so, one can change the output light as desired.

To count pulses we used a high precision comercial counter, GPIB controlled. Data acquisition and control is PC based. A LabView program was developped to integrate the motor and the GPIB control.

3.2 Long term stability

To check long term stability of the response against temperature changes, we have installed the setup inside a "climatic chamber". The distance between the LFC and the screen was kept fix (32 mm) along the experiment. The temperature in the chamber was first cooled down to about 7 °C, then warmed up to about 26 °C.

We have taken a total of 2500 measurements over 10 hours The time window was set to 1 s and the current at the LED was kept at 30 mA. The response as a function of the temperature can be seen in fig. 3. The response shows a linear dependence with the temperature. The number of pulses decreases for increasing temperature with a gradient of 0.45% $^{o}C^{-1}$. Data points are fitted to the following linear expression

$$S\ (\#\ pulses) = (-119.85 \pm 0.12)\ T\ (^{o}C) + (23568 \pm 24)$$

Fitted line in the figure is undistinguishable from the data points. To cross-check the above result we have repeated the experiment for a distance of 60 mm between the LFC and the screen, varying the temperature in the range 6 ^{o}C to 30 ^{o}C. The fitted function is now

$$S\ (\#\ pulses) = (-36.72 \pm 0.04)\ T\ (^{o}C) + (8823 \pm 1)$$

which corresponds to the same 0.45% $^{o}C^{-1}$ gradient.

3.3 Short distances measurements

We have studied the response of the device with the sensor-diffusion screen distance. The sensor was displaced towards the screen over the full range of the moving platform, from 60 mm to 35 mm. These distances fairly reproduce the maximum expected longitudinal motions range in CMS.

An integration method was used for signal readout. Accumulation of pulses over a long period of time (time window) is, in fact, an exposure measurement.

The measurements were done for three different time windows (0.25 s, 0.5 s and 1 s). In all three cases, the step was 0.25 mm (100 points measured), and the current at LED was 30 mA. The sensor-screen distance, given by the platform, is shown in fig. 4 as a function of the measured number of pulses, for the 1 s time window.

The shorter the distance is the higher the number of counts is for a given time window. In the example shown in fig. 4 the response varies from 82 pulses/mm at 60 mm to 378 pulses/mm at 35 mm.

For the three integration times, a polynomial function of order 7 in the counted pulses was necessary to fit the data. The fitted curve overlaps with the data points in fig. 4.

The results of the fits to the general form

$$D(mm) = \Sigma\ A_i\ x\ S^i \qquad (1)$$

where i runs from 0 to 7 and S comes in number of counted pulses, are given in table 1 for the three considered time windows.
To estimate the associated measuring resolutions we have calculated and distributed the residuals from the various fits. The measured resolutions (RMS of the distributions of the residuals) are: 16.1 μm, 15.3 μm and 7.9 μm for the 0.25 s, 0.50 s and 1 s time windows, respectively.
The higher the time window is the higher the integrated signal is and the better the resolution is.
Since the light intensity seen by the photosensor would be, for an ideal case, proportional to $1/D^2$, we have, for the 1 s time window example in fig. 4, fitted a function of the type

$$D(mm) = A/\sqrt{S} + B/S + C \qquad (2)$$

We obtain: A = 1575 ± 10, B = 142120 ± 500 and C = 11 ± 6, with a resolution of 55 μm which will be not enough for the foreseen application in CMS. Nevertheless, we expect that improving the device by increasing the mean response in the desired distance range it will be possible to calibrate the sensor with simple functions as that of eq. (2).

4. Summary and conclusions

A new, accurate and unexpensive device, consisting in an infrared light source and an infrared light to frequency converter, has been designed, constructed and used for short distance measurements. It has the advantages of a wide dynamic range of input light, immunity to noise and a minimum component interface.
Using an integration time of 1 s, distances in the range 35 to 60 mm are reconstructed with a resolution better than 10 μm.
In a near future, an improved device, having at least one order of magnitude higher response will be tested. For the particular application of short distance measurements in CMS, radiation hardness tests will be necessary.

References

[1] "The Large Hadron Collider Conceptual Design", The LHC Study Group, CERN/AC/95-05.
[2] "CMS: The compact Muon Solenoid Technical Proposal", G.L. Bayatian et al., CERN/LHCC 94-38.
[3] "CMS: The Magnet Project Technical Design Report", The CMS Collaboration, CERN/LHCC 97-10.
[4] "CMS: The Muon Project Technical Design Report", The CMS Collaboration, CERN/LHCC 97-32.

Table captions

Table 1: Fitted parameters in eq.(1) (see text) for 3 different time windows.

	0.25 s	0.50 s	1.00 s
A0	148.99 ± 0.29	147.71 ± 0.29	183.85 ± 0.29
A1	-0.58×10^{-1} ± 0.11×10^{-5}	-0.12 ± 0.23×10^{-5}	-0.51×10^{-1} ± 0.57×10^{-6}
A2	0.11×10^{-4} ± 0.22×10^{-9}	0.43×10^{-4} ± 0.93×10^{-9}	0.79×10^{-5} ± 0.59×10^{-10}
A3	-0.15×10^{-9} ± 0.41×10^{-13}	-0.15×10^{-8} ± 0.35×10^{-12}	-0.55×10^{-9} ± 0.56×10^{-14}
A4	-0.15×10^{-12} ± 0.73×10^{-17}	-0.23×10^{-11} ± 0.13×10^{-15}	-0.42×10^{-15} ± 0.51×10^{-18}
A5	-0.17×10^{-17} ± 0.12×10^{-20}	-0.20×10^{-15} ± 0.42×10^{-19}	0.25×10^{-17} ± 0.44×10^{-22}
A6	0.37×10^{-20} ± 0.18×10^{-24}	0.28×10^{-18} ± 0.13×10^{-22}	-0.14×10^{-21} ± 0.34×10^{-26}
A7	-0.26×10^{-24} ± 0.24×10^{-28}	-0.38×10^{-22} ± 0.35×10^{-26}	0.25×10^{-26} ± 0.23×10^{-30}

Table 1

Figure captions

Fig. 1: Block diagram of the working principle.

Fig. 2: Sketch of the setup.

Fig. 3: Response (in number of pulses) as a function of the temperature (in °C) for a fixed distance of 32 mm.

Fig.4: Distance as a function of the measured signal for 1 s time window.

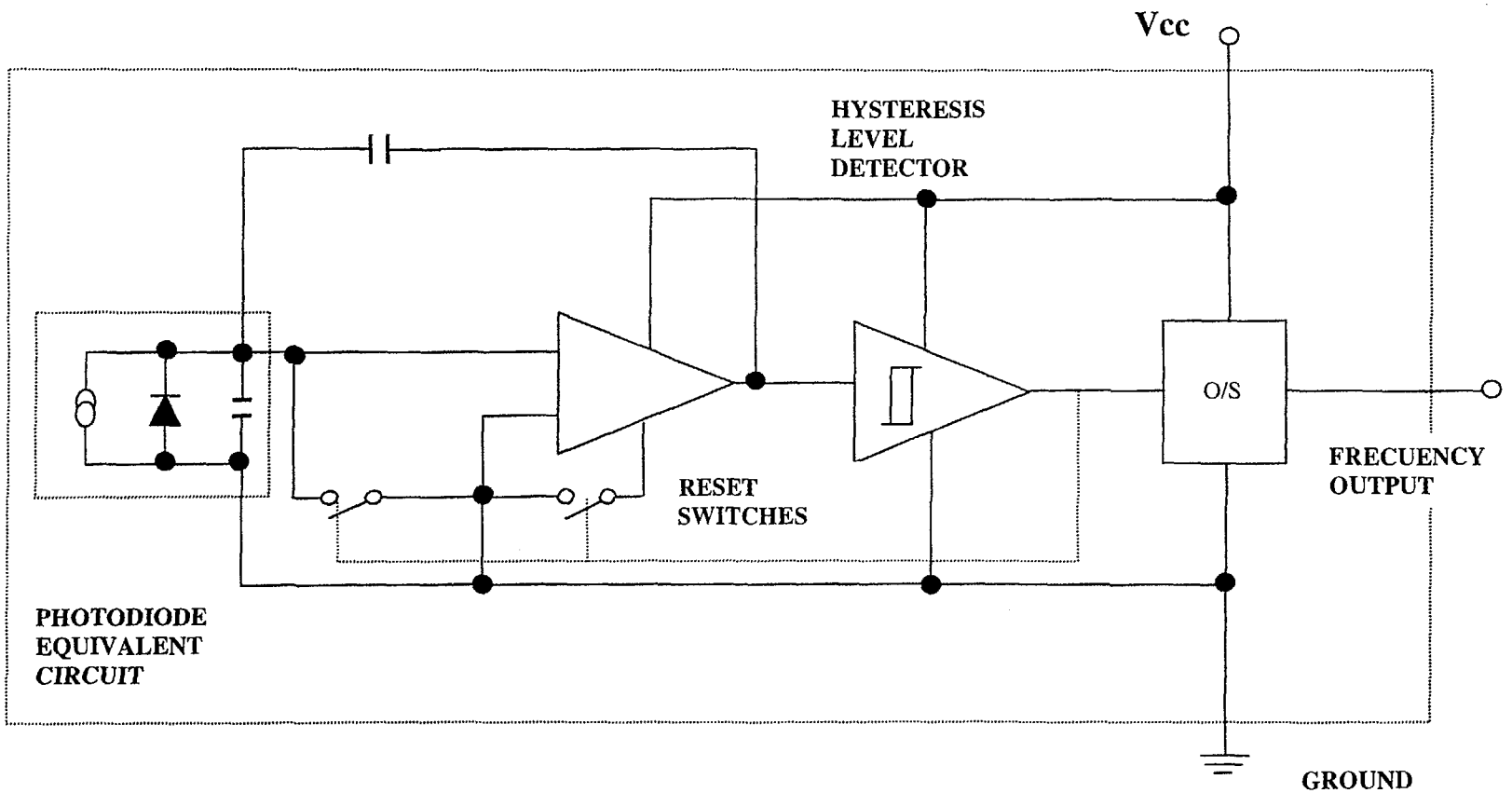
Vcc
HYSTERESIS
LEVEL
DETECTOR
O/S
FRECUENCY
OUTPUT
RESET
SWITCHES
PHOTODIODE
EQUIVALENT
CIRCUIT
GROUND

Fig. 1

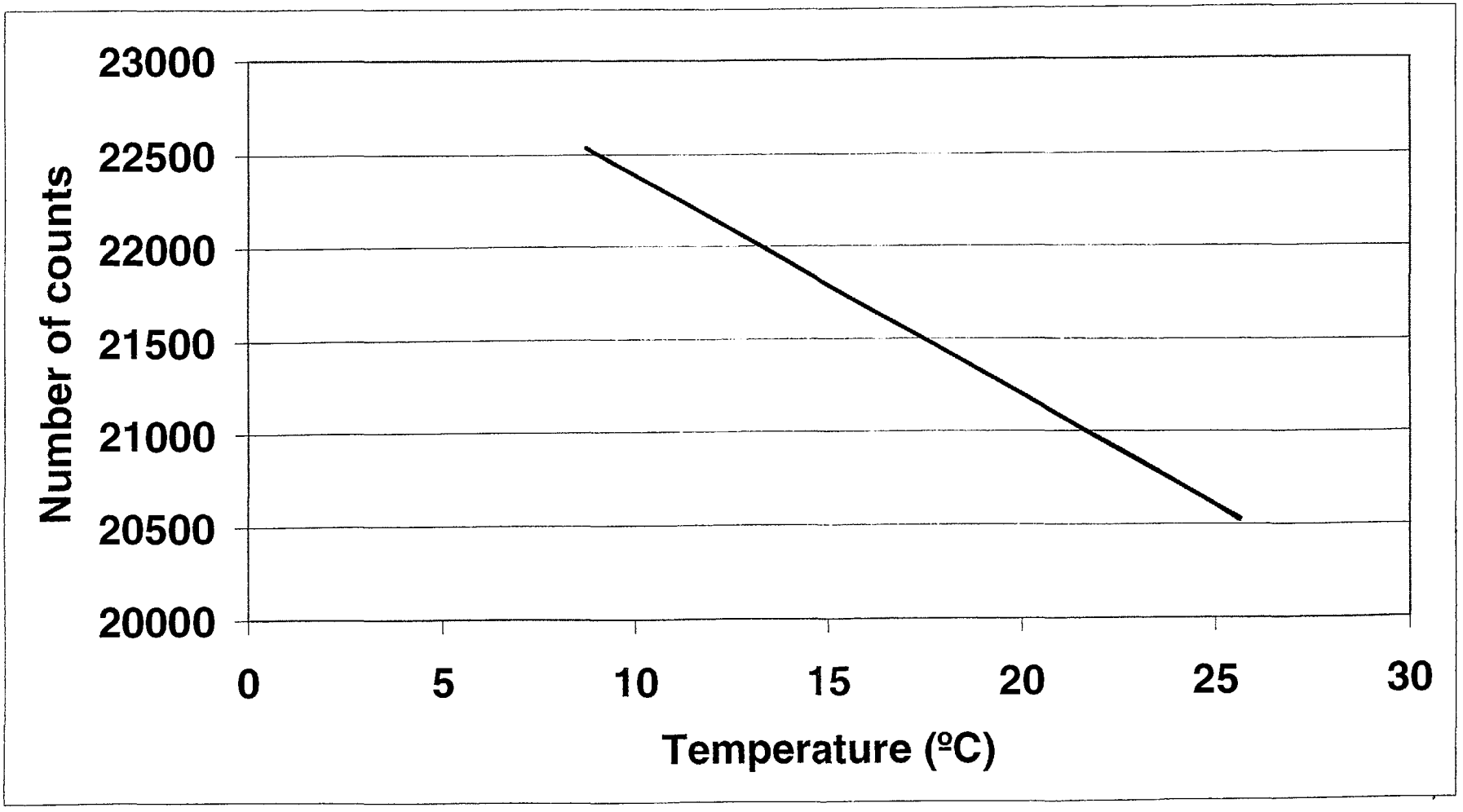
23000
22500
22000
21500
21000
20500
20000
Number of counts
0
5
10
15
20
25
30
Temperature (ºC)

Fig. 3

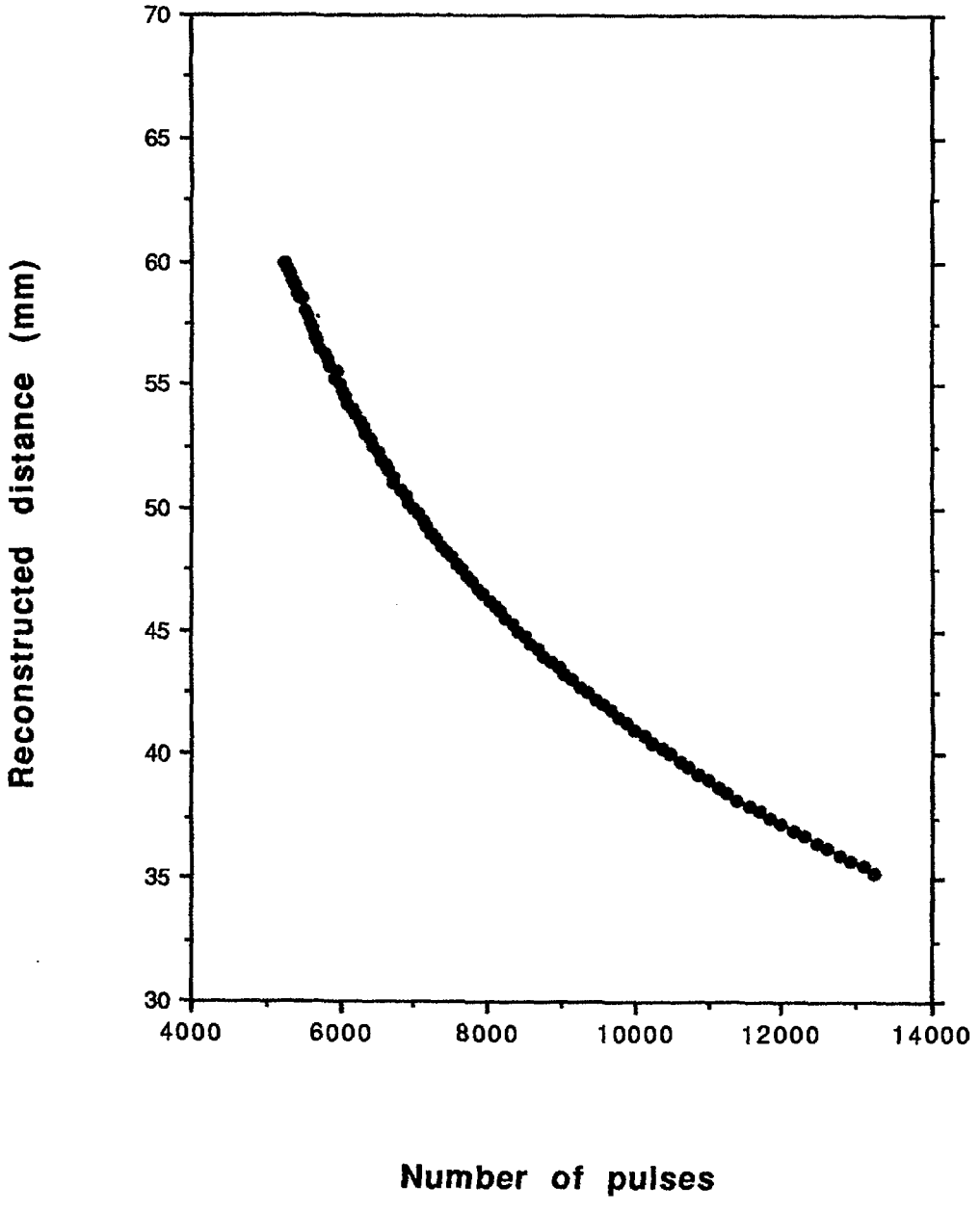
Reconstructed distance (mm)
70
65
60
55
50
45
40
35
30
4000
6000
8000
10000
12000
14000
Number of pulses

Fig. 4